Electronic Supplementary Information

Programmed Self-Assembly of Conjugated Oligomer-Based Helical Nanofibres through Hydrogen-Bonding Interactions

Yu Wang,[a+] Guoxin Yin,[a+] Pradeep Cheraku,[b+] Yu Xia,[a] Yuping Yuan,[a] Peng Miao,[c] Huidong Zang,[d] Mircea Cotlet,[d]* Ping Xu,[c]* Hsing-Lin Wang[a,b]*

a. *Department of Materials Science and Engineering, Southern University of Science and Technology, Xueyuan Avenue 1088, Shenzhen 518055, P. R. China*
b. *Physical Chemistry and Spectroscopy group, Chemistry Division, Los Alamos National Laboratory, Los Alamos, NM, 87545*
c. *Harbin Institute of Technology, 92 Xidazhi Street, Nangang, Harbin, Heilongjiang, P.R. China.*
d. *Center for Functional Nanomaterials, Brookhaven National Laboratory, Upton, New York 11973, United States.*

Email: wangxl3@sustech.edu.cn

Table of Contents

1. Molecular design

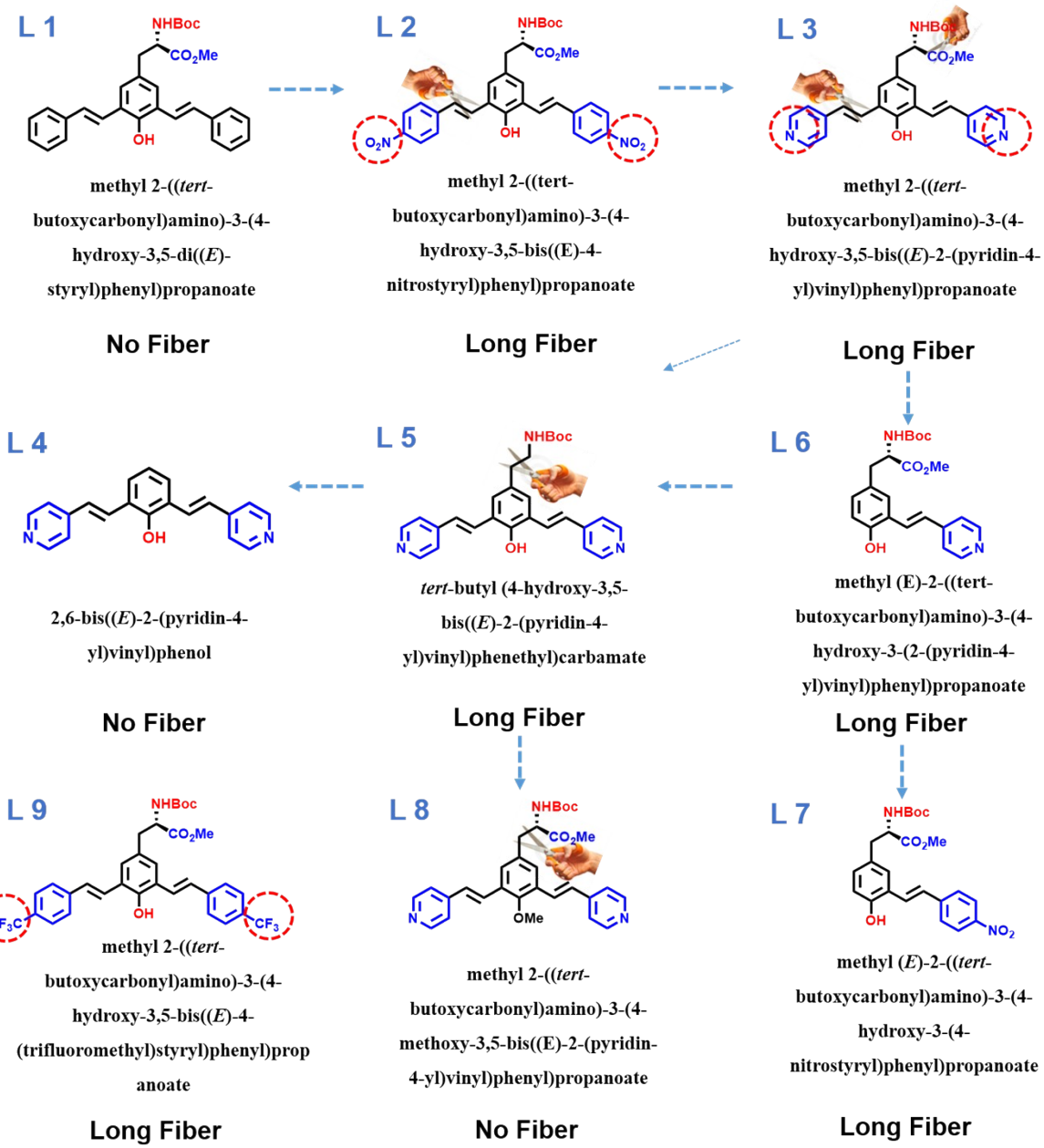

Fig. S1: Molecular design of our system. Molecular structures and corresponding name of L1-L9 used in this study. The self-assembled structures of L1-L9 are labelled. The attribution of functional groups in the assembly process can be understood.

2. Synthesis of L1 to L9

Molecules L1-L3, L6, L7, and L9 were synthesized according to our previous paper [1].

2.1 Synthesis of L 4

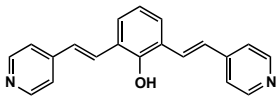

2.6-diiodophenol (500mg, 1.45mmol) and 4-vinylpyridine (0.31ml, 2.9mmol) were dissolved in 10ml N,N'-dimethylformamide and 10ml diisopropylethylamine in a flask. The mixture was bubbled with N_2 for 20min and palladium acetate (33.7mg, 0.15mmol) and tris(2-methylphenyl)phosphine (60.8mg, 0.2mmol) were added into the mixture under N_2 flow. The reaction was stirred at 100°C under N_2 for 24h. The reaction was cooled to room temperature and filtered through celite. The filtrate was collected and evaporated in vacuum. The crude product was purified by column chromatography with methanol/ethyl acetate (1/4, volume ratio) as eluent. After removing the solvent, 200mg white crystal was collected with yield of 46%. ^{1}H-NMR (400MHz, DMSO-d6), δ 9.65(s, 1H), 8.56(d, 4H, *J*=5.6Hz) 7.85(d, 2H, *J*=16.4Hz), 7.68 (d, 2H, *J*=4.0Hz), 7.56(d, 4H, *J*=6.0Hz), 7.21(d, 2H, *J*=16.4Hz), 6.98(t, 1H, *J*=5.6Hz); ^{13}C-NMR (100MHz, DMSO-d6), δ 153.31, 150.19, 145.42, 128.53, 127.57, 126.58, 125.60, 121.44, 121.12

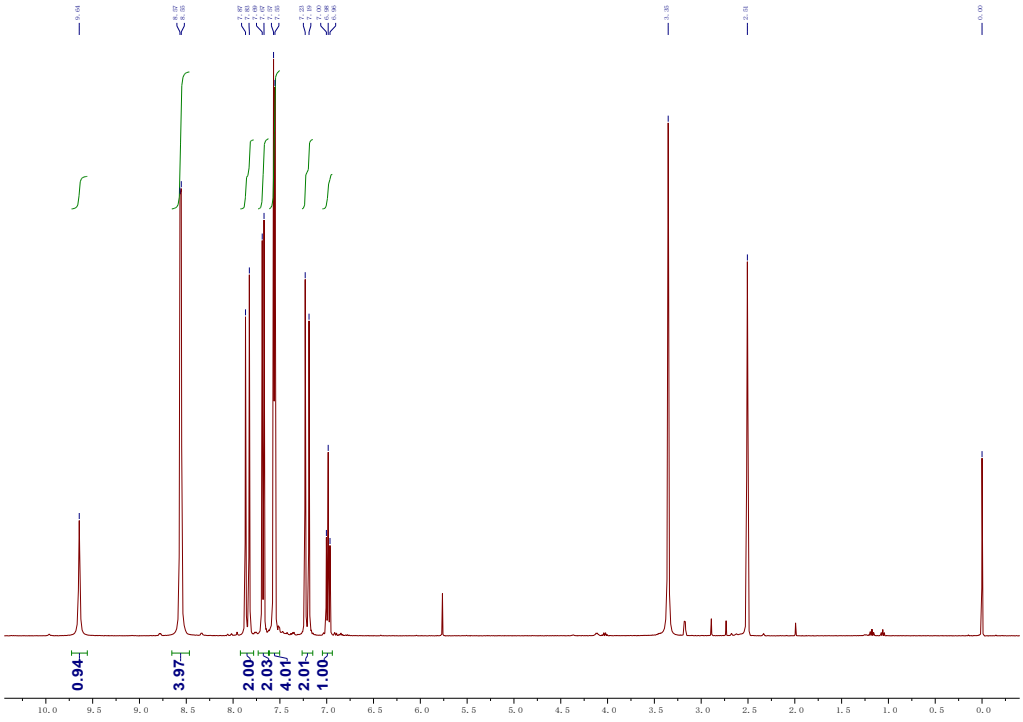

Fig. S2 ^{1}H-NMR (400MHz, DMSO-d6) spectrum of **L4**

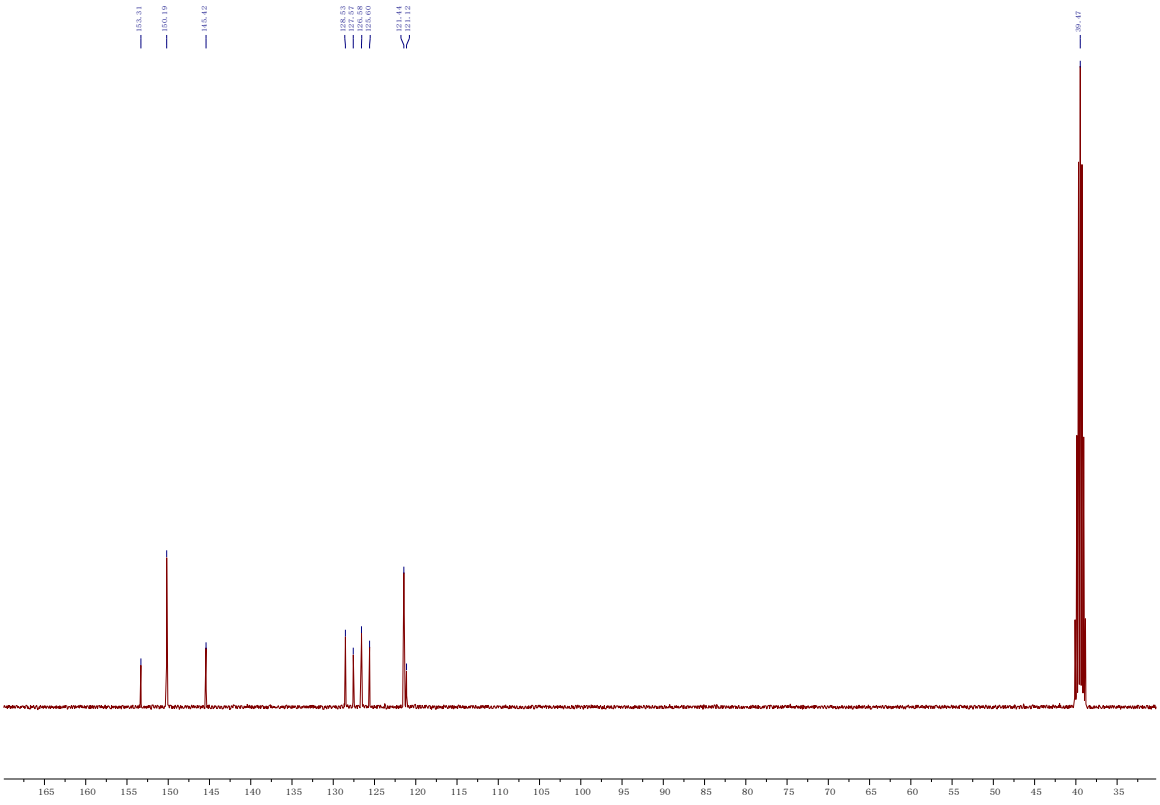

Fig. S3 ^{13}C-NMR (100MHz, DMSO-d6) spectrum of **L4**

2.2 Synthesis of L 5

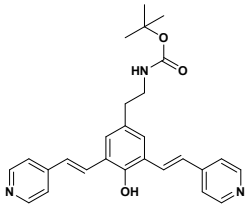

tert-butyl (3,5-diiodo-4-methoxyphenethyl)carbamate (540mg, 1.07mmol) and 4-vinylpyridine (0.23ml, 2.14mmol) were dissolved into the mixture of 10ml N,N'-dimethylformamide and 10ml diisopropylethylamine. The reaction mixture was bubbled with argon for 20 minutes to remove oxygen. Palladium acetate (24.0mg, 0.11mmol) and tris(2-methylphenyl)phosphine (45.6mg, 0.15mmol) were added into the mixture under N_2 flow. The reaction was stirred at 100°C under N_2 for 24h. The reaction was cooled to room temperature and filtered through celite. The filtrate was collected and evaporated in vacuum. The crude product was purified by column chromatography with methanol/ethyl acetate (1/9, volume

ratio) as eluent. After removing the solvent, 156.7mg off-white solid was collected with yield of 32%. ^{1}H-NMR (400MHz, DMSO-d6) δ 9.46(s, 1H), 8.56(d, 4H, *J*=5.2Hz), 7.82(d, 2H, *J*=16.4Hz) 7.56(d, 4H, *J*=5.6Hz), 7.51(s, 2H), 7.20(d, 2H, *J*=16.4Hz), 6.95(t, 1H, *J*=5.2Hz), 3.20(q, 2H, *J*=7.6Hz), 2.70(t, 2H, *J*=7.2Hz), 1.36(s, 9H); ^{13}C-NMR (100MHz, DMSO-d6), δ 156.05, 151.93, 150.52, 145.21, 131.55, 128.51, 127.63, 126.40, 125.35, 121.33, 77.97, 41.93, 35.21, 28.74

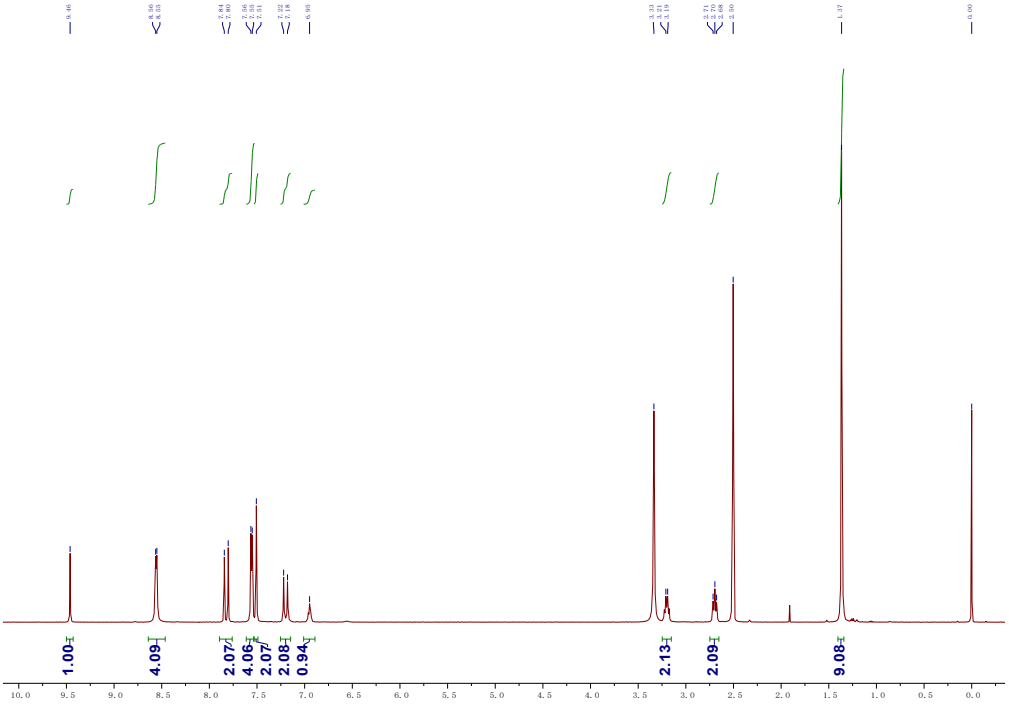

Fig. S4 ^{1}H-NMR (400MHz, DMSO-d6) spectrum of **L5**

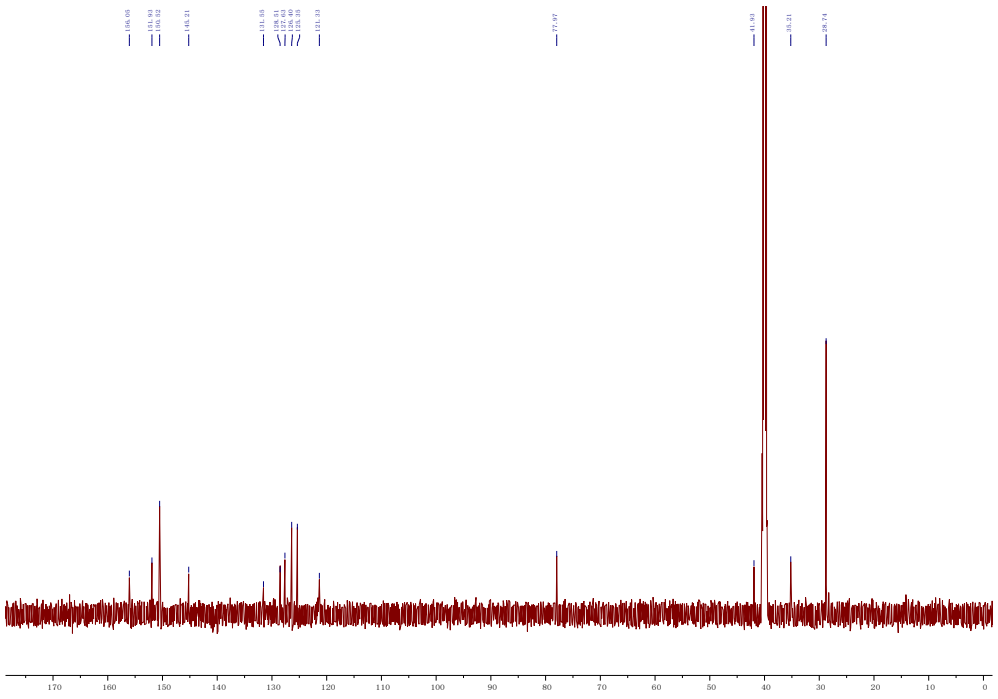

Fig. S5 ^{13}C-NMR (100MHz, DMSO-d6) spectrum of **L5**

2.3 Synthesis of L 8

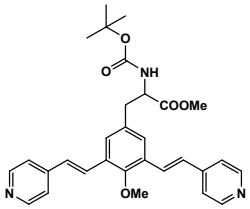

methyl 2-((tert-butoxycarbonyl)amino)-3-(3,5-diiodo-4-methoxyphenyl)propanoate (400mg, 0.71mmol) and 4-vinylpyridine (0.15ml, 1.42mmol) were dissolved into the mixture of 10ml N,N'-dimethylformamide and 10ml diisopropylethylamine. The reaction mixture was bubbled with argon for 20 minutes to remove oxygen. Palladium acetate (15.7mg, 0.07mmol) and tris(2-methylphenyl)phosphine (30.4mg, 0.1mmol) were added into the mixture under N_2 flow. The reaction was stirred at 100°C under N_2 for 24h. The reaction was cooled to room temperature and filtered through celite. The filtrate was collected and evaporated in vacuum. The crude product was purified by column chromatography with methanol/ethyl acetate (1/9, volume ratio) as eluent. After removing the solvent, 113.5mg off-white solid was collected with yield of 31%. ^{1}H-NMR (DMSO-d6, 400MHz) δ 8.63 – 8.57 (m, 4H), 7.73 (s, 2H), 7.65 (d, J = 16.5

Hz, 2H), 7.63 – 7.58 (m, 4H), 7.43 (d, J = 8.3 Hz, 1H), 7.31 (d, J = 16.5 Hz, 2H), 4.34 (dd, J = 5.0, 2.3 Hz, 1H), 3.12 (dd, J = 13.8, 4.8 Hz, 1H), 2.91 (dd, J = 13.8, 10.7 Hz, 1H), 1.31 (s, 9H).; 13C-NMR (DMSO-d6, 100MHz), δ 172.52, 155.40, 154.94, 150.16, 144.21, 133.89, 129.46, 128.00, 127.57, 126.74, 120.92, 78.30, 62.60, 54.93, 51.88, 36.06, 28.05

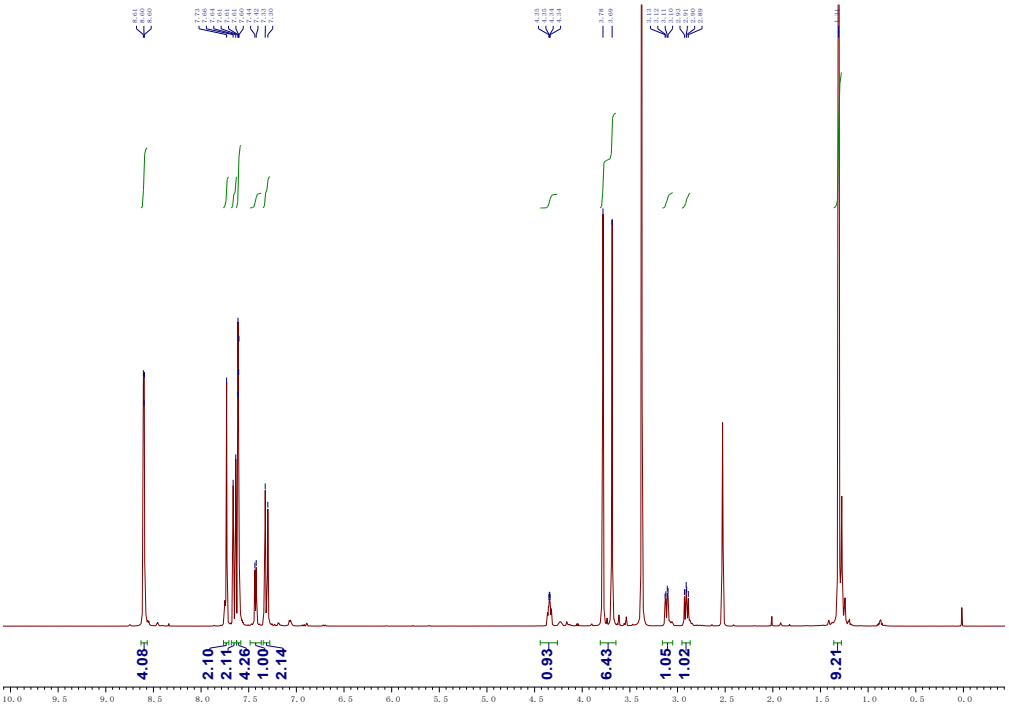

Fig. S6 ^{1}H-NMR (400MHz, DMSO-d6) spectrum of **L8**

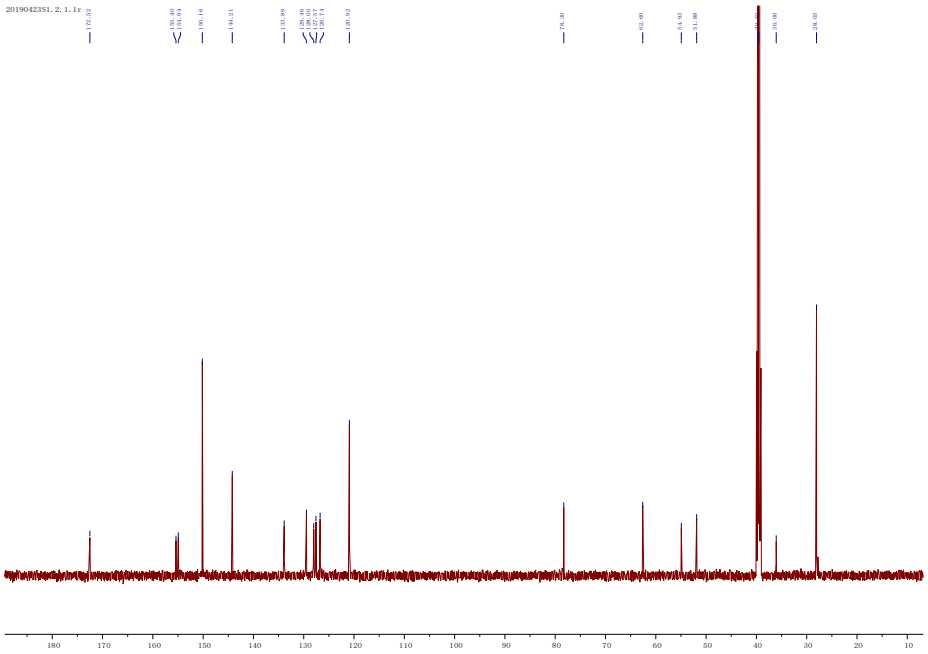

Fig. S7 ^{13}C-NMR (100MHz, DMSO-d6) spectrum of **L8**

3. Single Crystal Structure

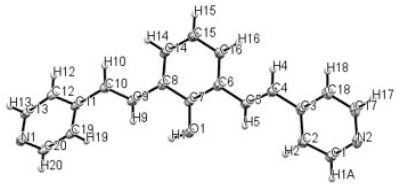

Fig. S8 Single crystal structure of L4. C, N and O atoms are shown as ellipsoids at the 50% probability level.

Table S1. Crystallographic data of L4.

Compound		L 6
Formula		$C_{20}H_{16}N_2O$
Space group		C2/c
Temperature (K)		100.0
Crystal system		monoclinic
Unit Cell Lengths (Å)	a	17.1908(14)
	b	6.0394(4)
	c	29.880(2)

Unit Cell angles (˚)	α	90
	β	104.899(3)
	γ	90
Cell Volume (Å3)		2998.0(4)
Z		8
Final R indices [I>2σ(I)]	R1	0.0507
	wR2	0.1145

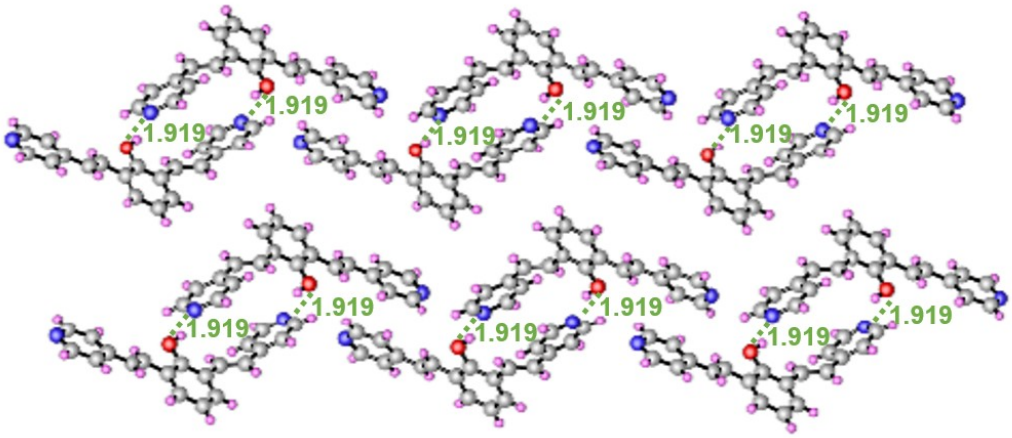

Fig. S9 Single crystal structure of L6 with interlocked dimer structure through intermolecular hydrogen bonding

4. DSC analysis of L2

The self-assembled nanofibres have higher melting point than that of pristine powder, which reveals the formation of strong and uniform hydrogen-bonding in the self-assembled structure. Hydrogen bonding interaction is stronger than other intermolecular interactions such as dipole−dipole attraction, π−π stacking, hydrophobic effect and electrostatic interaction. Therefore, self-assembled fibre with dominated hydrogen bonding interaction has larger melting point compared to the pristine powder without dominated hydrogen bonding interaction.

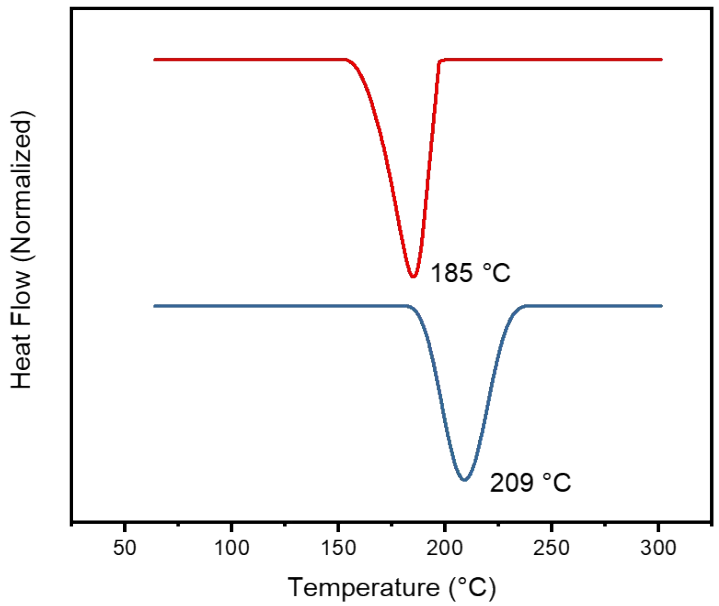

Fig. S10 Differential Scanning Calorimetry thermogram of the powder of L2 (red) and self-assembled fibre of L2 (blue).

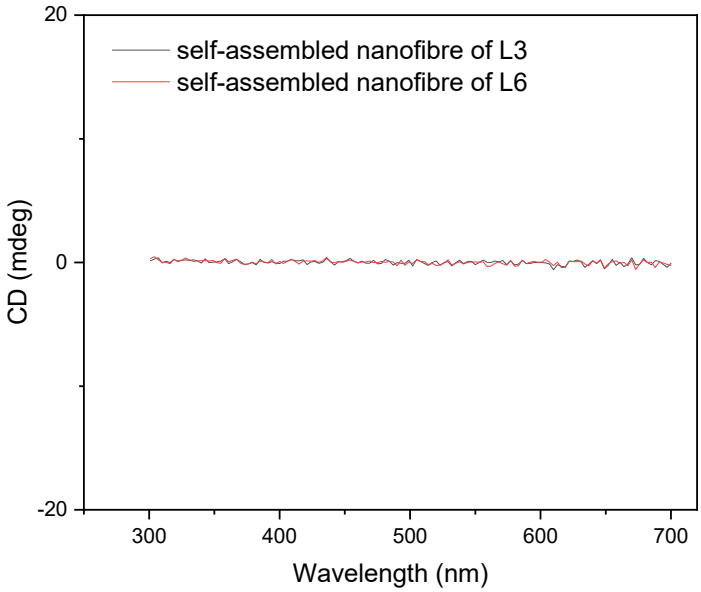

Fig. S11 CD spectra of the self-assembled fibers formed by L3 and L6.

5. Photo physical properties of self-assembled fibres

Fluorescence lifetime imaging microscopy (FLIM) has been used to reveal the lifetime of individual nanofibre and then ascertain the size/structure-dependent optical and photophysical properties. The FLIM mapping images that show lifetime of individual nanofibres denoted nanofibre 1 to 8 are shown in Fig. S11 and Fig. S13. By fitting the time-dependent attenuation (Fig S12(a) and Fig S13(c)), the lifetime of nanofibres was determined in Table S2 and S3. The monotonic increase in lifetime with decreasing nanofibre diameter suggests an increase in the number of nanofibres in each nanofibre bundle is an implication of nanofibre bundles has led to a smaller lifetime. It is particularly important to note that despite the difference in fibre diameter and fluorescence lifetime, the PL spectra of all these nanofibres are basically unchanged (Fig. 12S(b) and Fig. S13(d)) which suggests the overall chemical environment and interaction between chromophores remains unchanged.

Table S2. The parameter values of the kinetics of lifetime of single nanofibre in points 1-6.

	Amp Avg Lifetime	**Int Avg Lifetime**	**A_1**	**t_1**	**A_2**	**t_2**	χ^2	**Background**	**Diameter (μm)**
Fibre_1	0.5	0.83	1491.32	0.292	392.53	1.291	1.019	35.43	0.20
Fibre_2	0.38	0.59	435.41	1.078	2591.32	0.268	0.973	35.25	0.25
Fibre_3	0.3	0.38	5647.71	0.24	783.37	0.721	1.056	42.24	0.45
Fibre_4	0.33	0.46	829.4	0.826	4910.69	0.246	1.059	47.22	0.37
Fibre_5	0.34	0.46	772.65	0.826	4562.71	0.255	0.957	46.23	0.35
Fibre_6	0.29	0.35	1263.95	0.651	9379.59	0.245	1.113	47.93	1

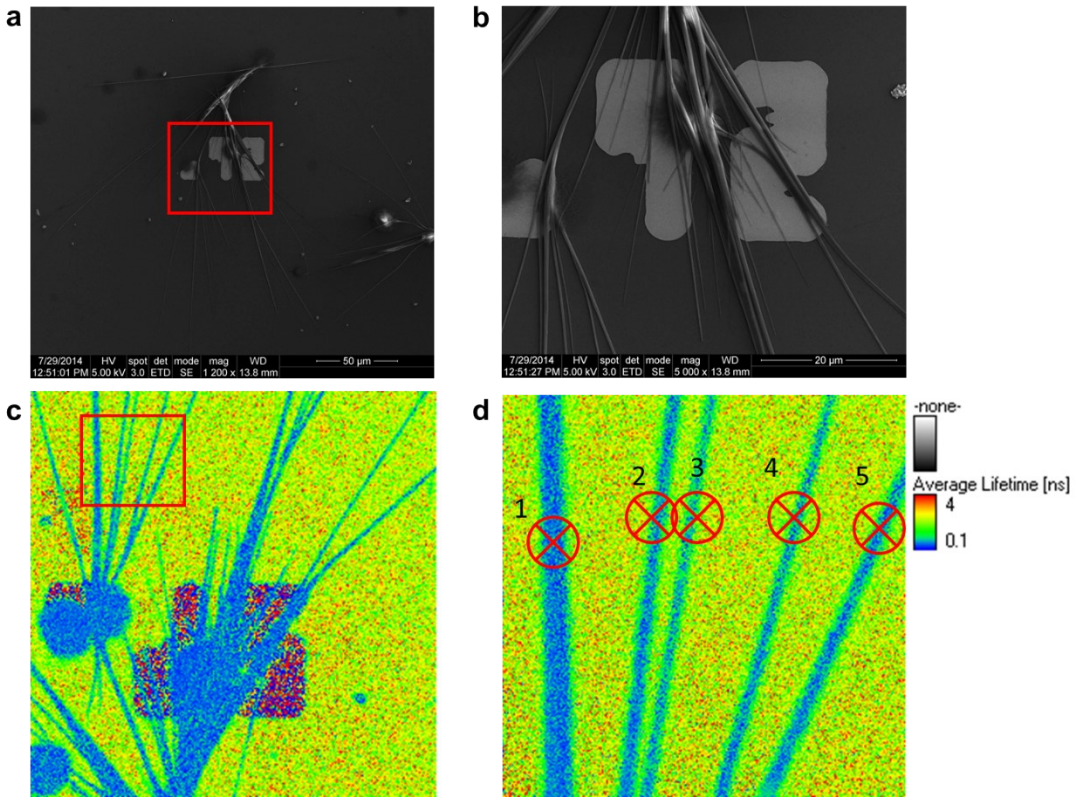

Fig. S12 SEM images (a)-(b) and fluorescence lifetime imaging (c)-(d) of nanofibre; Fluorescence lifetime imaging of single nanofibres in points 1-5.

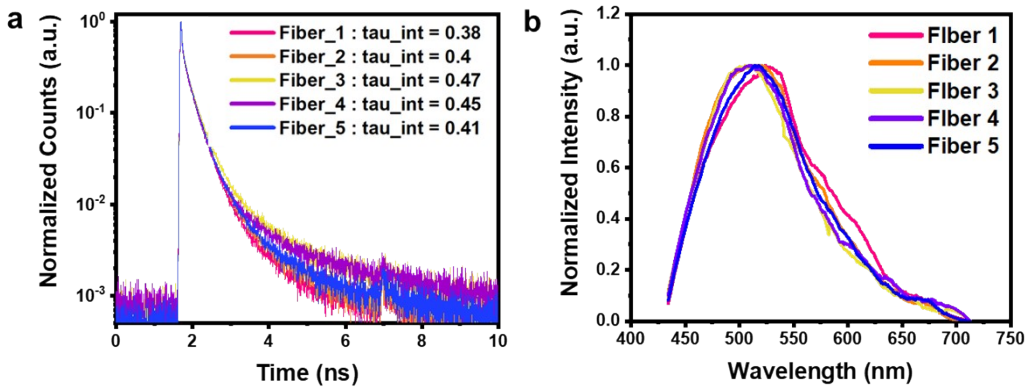

Fig. S13 (a) Lifetime and (b) Emission spectra of singe nanofibre in points 1-5.

Table S3. The parameter values of the kinetics of lifetime of single nanofibre in points 1-5.

	Amp Avg	Int Avg Lifetime	A_1	t_1	A_2	t_2	χ^2	Background	Diameter

	Lifetime								(μm)
Fibre_1	0.31	0.38	1709.69	0.68	10794.27	0.246	1.11	61.5	0.59
Fibre_2	0.32	0.4	1521.24	0.734	9578.19	0.25	1.141	61.21	0.35
Fibre_3	0.34	0.47	986.01	0.851	5746.76	0.256	1.126	56.13	0.24
Fibre_4	0.32	0.45	4651.54	0.249	608.52	0.889	0.986	44.39	0.32
Fibre_5	0.32	0.41	1337.56	0.747	8317.17	0.25	1.039	58.42	0.50

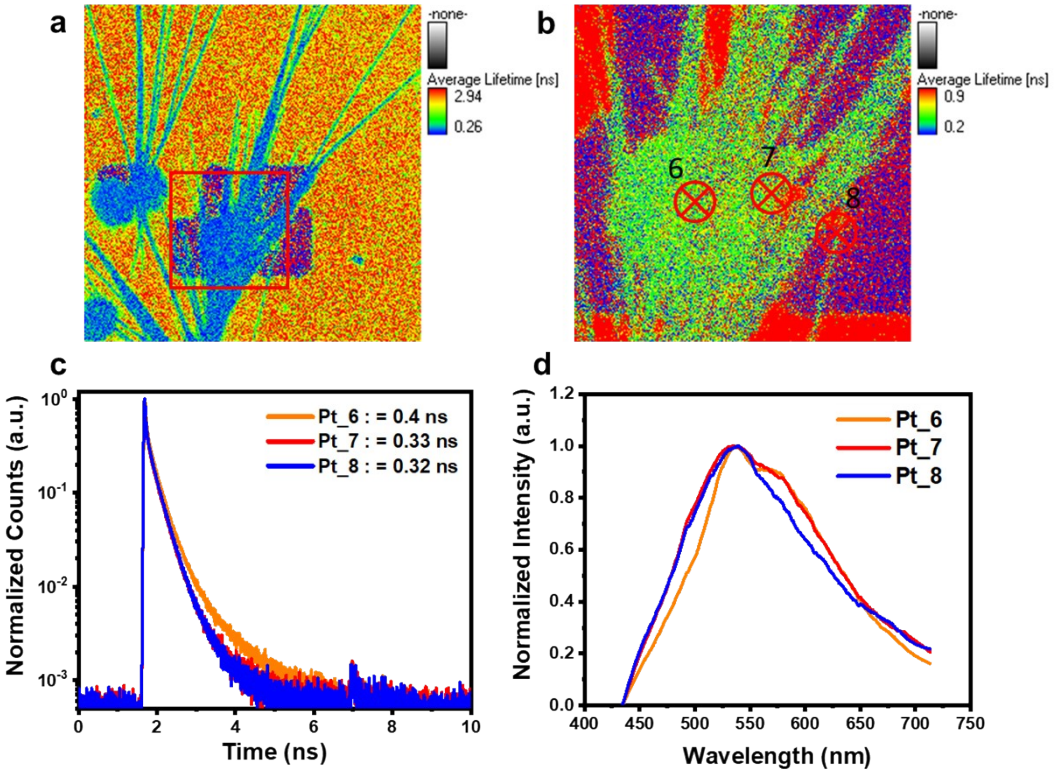

Fig. S14 (a)-(b) Fluorescence lifetime imaging of nanofibres; (c) Lifetime and (d) Emission spectra of singe nanofibre in points 6-8.

Table S4. The parameter values of the kinetics of lifetime of single nanofibre in points 6-8.

	Amp Avg Lifetime	Int Avg Lifetime	A_1	t_1	A_2	t_2	χ^2	Background	Diameter (μm)

Pt_6	0.31	0.4	2545.02	0.741	17117.01	0.249	1.285	98.64	0.50
Pt_7	0.28	0.33	1138.3	0.581	7517.38	0.237	1.025	37.92	1.29
Pt_8	0.28	0.32	1339.13	0.551	8451.52	0.239	0.994	41.02	1.35